Stokes parameters in the unfolding of an optical vortex through a birefringent crystal

Florian Flossmann, Ulrich T. Schwarz and Max Maier

Naturwissenschaftliche Fakultät II-Physik, Universität Regensburg, Universitätsstraße 31, D-93053 Regensburg, Germany

ulrich.schwarz@physik.uni-r.de

Mark R. Dennis

School of Mathematics, University of Southampton, Highfield, Southampton SO17 1BJ, UK

mark.dennis@soton.ac.uk

Abstract: Following our earlier work (F. Flossmann *et al.*, Phys. Rev. Lett. **95** 253901 (2005)), we describe the fine polarization structure of a beam containing optical vortices propagating through a birefringent crystal, both experimentally and theoretically. We emphasize here the zero surfaces of the Stokes parameters in three-dimensional space, two transverse dimensions and the third corresponding to optical path length in the crystal. We find that the complicated network of polarization singularities reported earlier – lines of circular polarization (C lines) and surfaces of linear polarization (L surfaces) – can be understood naturally in terms of the zeros of the Stokes parameters.

OCIS codes: (260.1440) Birefringence; (260.2110) Electromagnetic Theory; (260.5430) Polarization; (999.9999) Singular Optics

References and links

1. J. F. Nye, *Natural focusing and fine structure of light: caustics and wave dislocations*, IoP Publishing, 1999.
2. M. S. Soskin and M. Vasnetsov, "Singular optics," Prog. Opt. **42** 219–276 (2001).
3. J.F. Nye, "Lines of circular polarization in electromagnetic wave fields," Proc. R. Soc. Lond. A **389** 279–290 (1983).
4. M.R. Dennis, "Polarization singularities in paraxial vector fields: morphology and statistics," Opt. Commun. **213** 201–221 (2002).
5. M.V. Berry, "Singularities in waves and rays," in R. Balian, M. Kléman, and J.-P. Poirier, editors, *Les Houches Session XXV - Physics of Defects* (North-Holland, 1981).
6. K. O'Holleran, M.J. Padgett, and M.R. Dennis, "Topology of optical vortex lines formed by the interference of three, four and five plane waves," Opt. Express **14** 3039–3044 (2006).
7. M.V. Berry and M.R. Dennis, "Phase singularities in isotropic random waves," Proc. R. Soc. Lond. A **456** 2059–2079 (2000).
8. L. Allen, M. Beijersbergen, R.J.C. Spreeuw, and J.P. Woerdman, "Orbital angular momentum of light and the transformation of Laguerre-Gaussian laser modes, Phys. Rev. A **45** 8185–8189 (1992).
9. F. Flossmann, U.T. Schwarz, and M. Maier "Propagation dynamics of optical vortices in Laguerre-Gaussian beams," Opt. Commun. **250** 218–230 (2005).
10. R. Dorn, S. Quabis, and G. Leuchs, "Sharper focus for a radially polarized light beam," Phys. Rev. Lett. **91** 233901 (2003).
11. J.V. Hajnal, "Observation on singularities in the electric and magnetic fields of freely propagating microwaves," Proc. R. Soc. Lond. A **430** 413–421 (1990).

#75617 - $15.00 USD Received 29 September 2006; revised 31 October 2006; accepted 31 October 2006

12. A. Niv, G. Biener, V. Kleiner, and E. Hasman, "Manipulation of the Pancharatnam phase in vectorial vortices," Opt. Express **14** 4208–4220 (2006).
13. M.V. Berry and M.R. Dennis, "The optical singularities of birefringent dichroic chiral crystals," *Proc. R. Soc. Lond. A* **459** 1261–1292 (2003).
14. M.V. Berry and M.R. Jeffrey, "Conical diffraction: Hamilton's diabolic point at the heart of crystal optics," Prog. Opt. in press.
15. Y. A. Egorov, T. A. Fadeyeva, and A. V. Volyar, "Fine structure of singular beams in crystals: colours and polarization," *J. Opt. A: Pure Appl. Opt.* **6** S217–S228 (2004).
16. F. Flossmann, U. T. Schwarz, M. Maier, and M. R. Dennis, "Polarization singularities from unfolding an optical vortex through a birefringent crystal," Phys. Rev. Lett. **95** 253901 (2005).
17. B. Riemann, in *Bernhard Riemann's gesammelte mathematische Werke und wissenschaftlicher Nachlass*, edited by H. Weber (Teubner, Leipzig, 1892) p. 301.
18. R.M.A. Azzam and N.M. Bashara, *Ellipsometry and polarized light* (North-Holland, 1977).
19. D.S. Kliger, J.W. Lewis, and C.E. Randall, *Polarized light in optics and spectroscopy* (Academic Press, San Diego, 1990).
20. I. Freund, A.I. Mokhun, M.S. Soskin, O.V. Angelsky, and I.I. Mokhun, "Stokes singularity relations," Opt. Lett. **27** 545–547 (2002).
21. D.J. Struik, *Lectures on Classical Differential Geometry* (Dover, 1988).
22. A. Volyar, V. Shvedov, T. Fadeyeva, A.S. Desyatnikov, D.N. Neshev, W. Krolikowski, and Y.S. Kivshar, "Generation of single-charge optical vortices with an uniaxial crystal" Opt. Express **14** 3724–3729 (2006).
23. M.R. Dennis, "Braided nodal lines in wave superpositions," New J. Phys. **5** 134 (2003).
24. F. Flossmann, *Singularitäten von Phase und Polarisation des Lichts* (PhD Thesis, University of Regensburg, 2006).

1. Introduction

Singular optics is an important branch of modern optics. In scalar optics, this is the study of optical vortices (phase singularities, or wave dislocations) [1, 2] and in polarization optics, polarization singularities (C points and lines, L lines and surfaces) [3, 4]. These singularities are geometric organizing centers in spatially extended optical fields which naturally arise in the propagation, interference and diffraction of optical fields [5], and the 2- and 3-dimensional singularity geometry reveals features of the underlying optical wave physics.

Optical vortices are generalized interference fringes, and generically occur whenever three or more waves are superposed [6], as well as in speckle patterns [7] and in beams carrying orbital angular momentum, such as Laguerre-Gauss (LG) beams [8, 9]. They are places (points in two dimensions, lines in three) where the scalar amplitude is zero, and in a loop around which the phase changes by $\pm 2\pi n$, where n is the integer vortex strength (charge).

Polarization singularities are places in coherent elliptic polarization fields where geometric polarization parameters cannot be mathematically defined. They are important in understanding the fine structure of beams whose polarization is spatially inhomogeneous, and their presence can give rise to significant physical effects [10]. The polarization singularities which propagate stably in paraxial beams are C lines of circular polarization, where the major axis of the polarization ellipse is not defined, and L surfaces of linear polarization, where polarization handedness is not defined. These appear as C points and L lines respectively in the transverse plane. Polarization singularities occur in fields evolving from waveguides [11], polarization-varying micrograting [12], and light propagating through anisotropic media [13, 14, 15].

In Ref. [16], a physical connection between the optical vortices of scalar optics and polarization singularities of vector optics was investigated. A linearly polarized LG_0^1 beam with an on-axis vortex propagated through a birefringent crystal, and the outgoing polarization structure was interpreted in three dimensions (two transverse and a third, the optical thickness of the crystal, effectively a phase shift). It was found that the crystal birefringence unfolds the input optical vortex into to a complicated network of polarization singularities. A pair of C lines, of opposite index and handedness, forms a double helix structure, intertwined around an L surface, which is topologically identical to the periodic minimal surface known as Riemann's examples

#75617 - $15.00 USD Received 29 September 2006; revised 31 October 2006; accepted 31 October 2006

or Riemann's minimal surface [17]. This pattern of singularities arises from the breaking of symmetries of the input beam (uniform linear polarization, intensity cylindrically symmetric) due to the anisotropy of the crystal.

The standard description of optical polarization employs the Stokes parameters, and their geometric representation on the Poincaré sphere. Here, we describe the behavior of Stokes parameters in the unfolding of a linearly polarized optical vortex beam through a birefringent crystal, and find that features of the polarization singularity geometry reported in Ref. [16] have a natural interpretation in terms of the zero contour surfaces of the Stokes parameters. We also present new experimental results on the structure of polarization singularities stemming from the unfolding of Gaussian beams with no vortices and higher order vortices on propagating through the crystal.

2. Interpretation using Stokes Parameters

Any state of paraxial, elliptic polarization can be described completely using the Stokes parameters [18, 19]. The complex electric field vector $\mathbf{E} = (E_x, E_y)$ describes the polarization ellipse, parameterized by its overall size (intensity), angle of major axis α, and a shape parameter ω, defined such that $|\tan\omega|$ is the ratio of minor and major ellipse axes, and $\operatorname{sign}\omega$ is the ellipse handedness (see Figure 1(a)). Up to a phase factor, the polarization vector is therefore

$$\begin{aligned} \mathbf{E} &= \sqrt{I}(\cos\omega\cos\alpha - i\sin\omega\sin\alpha, \cos\omega\sin\alpha + i\sin\omega\cos\alpha) \\ &= \sqrt{I}(\cos\beta\exp(-i\delta), \sin\beta\exp(i\delta)), \end{aligned} \tag{1}$$

where I is the overall intensity $|\mathbf{E}|^2$, α and ω are the ellipse parameters, and β and δ are a pair of equivalent parameters [19], which prove to be more useful in our analysis. The unnormalized Stokes parameters are defined [18, 19]

$$\left.\begin{array}{llll} S_0 = |E_x|^2 + |E_y|^2, & = I, & & \\ S_1 = |E_x|^2 - |E_y|^2 & = I_{0^\circ} - I_{90^\circ} & = I\cos 2\alpha\cos 2\omega & = I\cos 2\beta, \\ S_2 = E_x^* E_y + E_x E_y^* & = I_{45^\circ} - I_{135^\circ} & = I\sin 2\alpha\cos 2\omega & = I\sin 2\beta\cos 2\delta, \\ S_3 = -i(E_x^* E_y - E_x E_y^*) & = I_{\mathrm{rhcp}} - I_{\mathrm{lhcp}} & = I\sin 2\omega & = I\sin 2\beta\sin 2\delta. \end{array}\right\} \tag{2}$$

The terms in the third column denote the intensity of the scalar component of a particular polarization determined with the appropriate analyzer. The third set is in terms of the ellipse parameters α, ω, and the third, the complementary parameters β, δ. Since $S_0^2 = S_1^2 + S_2^2 + S_3^2$, any state of polarization can be represented on the surface of a sphere, with coordinates S_i/S_0 $(i = 1, 2, 3)$ – this is the Poincaré sphere (Figure 1). From Eq. (2), angles 2α and 2ω are the azimuth and colatitude angles on the Poincaré sphere with S_3 as the axis. δ and β may be understood as the corresponding half-angles for azimuth and latitude with respect to S_1 as the axis. Physically, S_0 is simply the field intensity I, and $S_3/S_0 = \sin 2\omega$ is the ellipticity, signed by handedness: positive for right-handed elliptical polarization, negative for left-handed. When $S_3 = 0$, the polarization is linear, so the zero contour surface of S_3 is the L surface [1, 4, 20]. The angle $\alpha = \arg(S_1 + iS_2)/2$ is the angle of the polarization ellipse major axis, and is undefined when $S_1 = S_2 = 0$; this is the condition for circular polarization (where $\omega = \pm\pi/2, |S_3| = S_0$). The polarization singularity positions are therefore determined by the zero surfaces of the three Stokes parameters: L surfaces by $S_3 = 0$, and C lines by the intersection of the surfaces $S_1 = 0$ and $S_2 = 0$.

The polarization phenomena described here are the result of a spatially inhomogeneous, linearly polarized monochromatic optical beam propagating through a birefringent crystal, and depend on three birefringence effects: the incident polarization is resolved into the two characteristic linear polarizations corresponding to that propagation direction; each of these two rays

#75617 - $15.00 USD Received 29 September 2006; revised 31 October 2006; accepted 31 October 2006

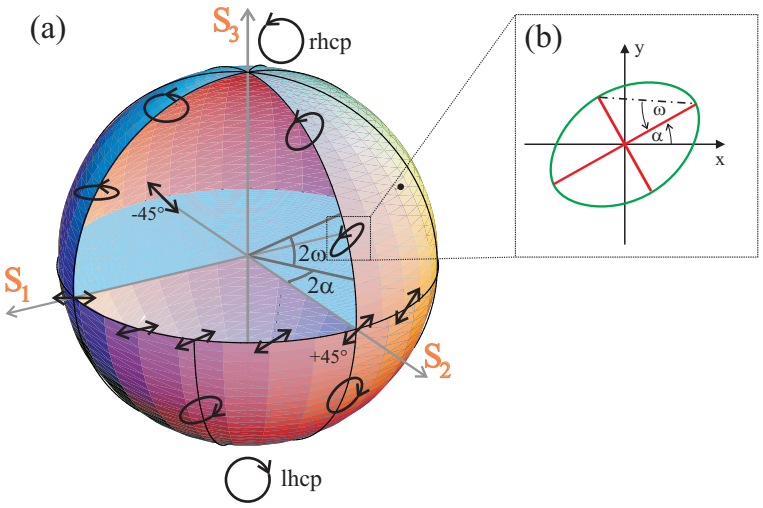

Fig. 1. (a) Representation of the Poincaré sphere. In abstract three-dimensional space, the Stokes parameters are Cartesian axes for a sphere, whose points represent states of elliptic polarization. 2α and 2ω are the azimuth and colatitude angles respectively for spherical coordinates with S_3 as the axis. Not shown are 2δ and 2β, which are the azimuth and latitude angles for spherical coordinates with S_1 as the axis. (b) Representation of the ellipse parameters. α is the angle of the major axis, ω the arctangent of the ratio of minor and major axes (signed by handedness).

propagates with a particular speed, resulting in a net phase shift between the two; beam walkoff results in a transverse spatial separation of the two rays. The incident propagation direction is taken not to be close to the optic axes of the crystal, so the effect of conical diffraction [14] may be ignored, as well as whether the crystal is uniaxial or biaxial. The details of our experiment, involving uniaxial KDP, are described in Ref. [16]; they are summarized in Fig. 2. The Gaussian beam (with waist width w_0) is incident in the plane containing the surface normal and the optic axis, implying that the spatial shift between the two beam components is in the direction of one of the crystal eigenpolarizations, and the difference in geometrical path length is negligible compared to the difference in optical path length. The phase shift therefore arises from the difference in refractive index, i.e. $\Lambda = 2\pi(n_2 - n_1)l/\lambda_{\text{vac}}$, where l is the average path length of the two rays. We will comment in the final section on what happens for crystals with optical activity and absorption, but in our experiment, these effects are negligible.

Following the notation of Ref. [16], the uniformly polarized beam incident on the crystal is $\mathbf{E}_{\text{in}}(x,y) = \psi(x,y)\mathbf{d}_{\text{in}}$, where $\psi(x,y)$ is the complex scalar amplitude of the incident field, and $\mathbf{d}_{\text{in}}$ is a unit vector representing the initial polarization, written in terms of β_{in} and δ_{in} by appropriate modification of Eq. (1). In the crystal, the two polarizations which propagate in the crystal are $\mathbf{d}_1, \mathbf{d}_2$ (defined to be in the x,y-directions), the path length-dependent phase shift is Λ and transverse shifts (in the x-direction) $\pm s$ result in a total outgoing field

$$\begin{aligned} \mathbf{E}(x,y,\Lambda) &= \sum_{j=1,2} \psi(x+(-1)^j s, y)(\mathbf{d}_{\text{in}} \cdot \mathbf{d}_j)\mathbf{d}_j \exp(i(-1)^j \Lambda/2) \qquad (3) \\ &= \left(\psi(x-s,y)\cos\beta_{\text{in}} \exp(-i[\Lambda/2+\delta_{\text{in}}]), \psi(x+s,y)\sin\beta_{\text{in}} \exp(i[\Lambda/2+\delta_{\text{in}}])\right). \end{aligned}$$

#75617 - $15.00 USD Received 29 September 2006; revised 31 October 2006; accepted 31 October 2006

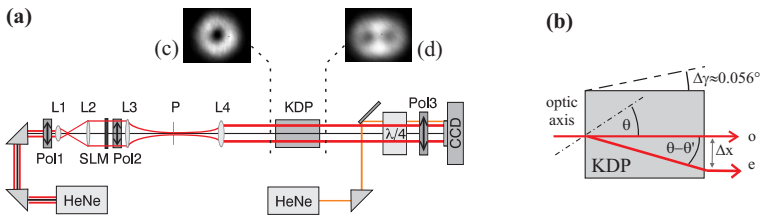

Fig. 2. (a) Experimental setup scheme. A beam with uniform polarization $\mathbf{d}_{\rm in}$ and varying complex amplitude $\psi(x,y)$ (incorporating a Gaussian factor with waist width $w_0 = 0.7\,$mm), is synthesized from a He–Ne laser using the polarizer Pol2 and spatial light modulator SLM. Higher diffraction orders are removed by a telescope (lenses L3 and L4) and a pinhole P. The KDP birefringent crystal is located in the waist plane. The Stokes parameters for each outgoing x,y are measured by a CCD camera using different combinations of the polarizer Pol3 and $\lambda/4$–plate. A second laser propagating through the analyser gives a fixed reference point. (b) Orientation of crystal, and ordinary and extraordinary rays (angles are exaggerated). The normal to the crystal surface is initially in the z-direction, and the optic axis is the xz-plane. Λ is varied by rotating the crystal about the y–axis, which does not change the polarizations $\mathbf{d}_{1,2}$. Typically two Λ–periods are measured, corresponding to $\Delta\gamma = 0.112^\circ$. (c) and (d) Intensity profiles of input and outgoing beams.

The Stokes parameters of the outgoing field are easily computed, where $\psi_\pm = \psi(x \pm s, y)$:

$$\begin{aligned} S_0 &= |\psi_-|^2 \cos^2\beta_{\rm in} + |\psi_+|^2 \sin^2\beta_{\rm in} \\ S_1 &= |\psi_-|^2 \cos^2\beta_{\rm in} - |\psi_+|^2 \sin^2\beta_{\rm in} \\ S_2 &= \sin 2\beta_{\rm in} \left({\rm Re}\{\psi_-^* \psi_+\} \cos(\Lambda + 2\delta_{\rm in}) + {\rm Im}\{\psi_-^* \psi_+\} \sin(\Lambda + 2\delta_{\rm in}) \right) \\ S_3 &= \sin 2\beta_{\rm in} \left(-{\rm Re}\{\psi_-^* \psi_+\} \sin(\Lambda + 2\delta_{\rm in}) + {\rm Im}\{\psi_-^* \psi_+\} \cos(\Lambda + 2\delta_{\rm in}) \right) \end{aligned} \qquad (4)$$

By inspection of these equations, the following observations can be made:

- S_0 and S_1 are independent of Λ (since the only Λ-dependence in Eq. (3) is in the phase of the two Cartesian components);
- At $x = \pm s, y = 0$, $S_1 \neq 0$, but $S_2 = S_3 = 0$;
- The only effect of shifting $\delta_{\rm in}$ is effectively to shift Λ;
- S_2, S_3 are identical, except for a quarter-period Λ-shift.

The final two points can be understood by interpreting the effect of a quarter-period phase difference as the effect of an appropriately oriented quarter-wave plate, which does not change S_1, but transforms S_2 to S_3, and S_3 to $-S_2$. In Stokes space, this is illustrated by a rotation of the Poincaré sphere by $\pi/2$ about the S_1-axis, corresponding to a change of $\pi/4$ in δ. This is represented in Fig. 3, in which experimental plots are compared for $\mathbf{d}_{\rm in}$ oriented at 45° (Fig. 3(a)) and right handed circular polarized (Fig. 3(b)), where $\delta_{\rm in}$ differs $\pi/4$ and Λ by $\pi/2$. On changing Λ by π, the pattern changes in a way analogous to a half-wave plate (as observed in Ref. [16]), namely S_1 is unchanged, but S_2 and S_3 change sign.

The comments above apply for any input field $\psi(x,y)$. In Ref. [16], this was chosen to be a Gaussian beam carrying a strength 1 on-axis optical vortex (i.e. a Laguerre-Gauss LG_0^1 mode), so $\psi_1 = (x+iy)\exp(-(x^2+y^2)/w_0^2)$. The polarization singularities are determined by the zero

#75617 - $15.00 USD Received 29 September 2006; revised 31 October 2006; accepted 31 October 2006

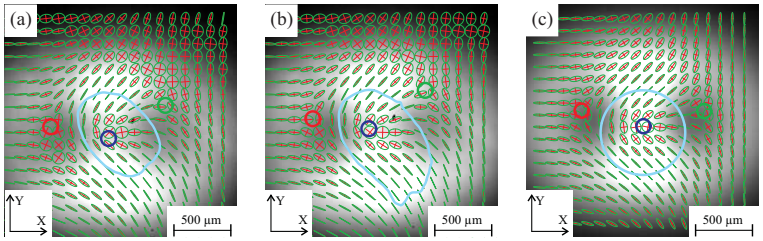

Fig. 3. The polarization field for a constant phase shift Λ, for an input beam $\psi = (x+iy)\exp(-(x^2+y^2)/w_0^2)$. Background intensity is the output intensity S_0, the small ellipses represent the polarization state (as in Fig. 1(b)), with C points of circular polarization represented by colored circles, the L line of linear polarization by a blue curve. (a) Input linear polarization with $\alpha_{\rm in} = \beta_{\rm in} = 45^\circ, \delta_{\rm in} = 0^\circ$ and $\Lambda = \pi + 0.1$. (b) Input circular polarization with $\beta_{\rm in} = \delta_{\rm in} = 45^\circ$, and $\Lambda = \pi/2 + 0.1$. (c) Theoretical plot for the situation represented in (a) and (b), based on Eq. (3).

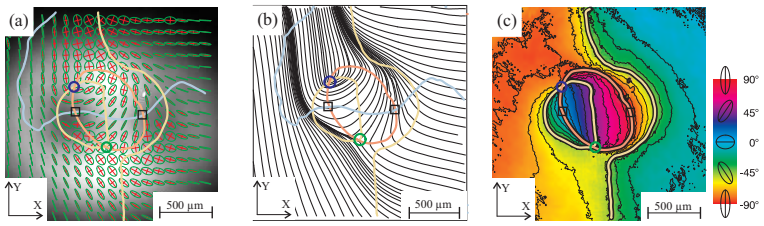

Fig. 4. Representations of the experimentally-determined polarization field for fixed $\Lambda = 0$, with Stokes parameter zero contours (light brown $S_1 = 0$, dark orange $S_2 = 0$, light blue $S_3 = 0$). The $S_1, S_2 = 0$ lines intersect at C points, represented by colored circles, and the $S_2, S_3 = 0$ lines intersect at the positions of the refracted vortices $x = \pm s, y = 0$. (a) Intensity and ellipse field. (b) Polarization streamlines. The curve tangent at each point represents the ellipse axis orientations α. (c) Orientation of ellipse axis α as hue plot. The singular nature of the C points, with index $\pm 1/2$, is exhibited clearly in (b) and (c), where α is not defined.

loci of the Stokes parameters S_1, S_2, S_3. Using Eq. (4), the zeros occur at the following x, y, Λ-coordinates (where, for simplicity here and hereafter, $\delta_{\rm in} = 0$) :

$$\left.\begin{array}{lll} S_1: & \frac{(x-s)^2+y^2}{(x+s)^2+y^2}\exp(8sx/w_0^2) & = \tan^2\beta_{\rm in} \\ S_2: & x^2+(y+s\tan\Lambda)^2 & = s^2\sec^2\Lambda \\ S_3: & x^2+(y-s\cot\Lambda)^2 & = s^2\,\mathrm{cosec}^2\,\Lambda \end{array}\right\} \text{ charge 1 vortex input.} \qquad (5)$$

(The equations for $S_2, S_3 = 0$ assume that $\sin 2\beta \neq 0$, i.e. $\mathbf{d}_{\rm in} \neq \mathbf{d}_1$ or $\mathbf{d}_2$.) As expected, the $S_1 = 0$ surface is independent of Λ. The solution for x and y is transcendental, depending only on the input $\beta_{\rm in}$ and the splitting s. On the other hand, the surfaces $S_2 = 0$ and $S_3 = 0$ are independent of $\beta_{\rm in}$, and are mathematically easily determined: each constant-Λ section is a circle, with radius $|(\mathrm{co})\sec\Lambda|$ and center $x = 0, y = (\mathrm{co})\tan\Lambda$. Such a circle for $S_3 = 0$ is plotted as the L line in Fig. 3(c); the experimental results, although topologically the same, do not give circles, probably due to lack of perfect rotational symmetry of the input beam. Various representations of the experimentally-determined ellipse parameters and zero contours of Stokes parameters, for a fixed choice of Λ, are plotted in Fig. 4.

#75617 - $15.00 USD Received 29 September 2006; revised 31 October 2006; accepted 31 October 2006

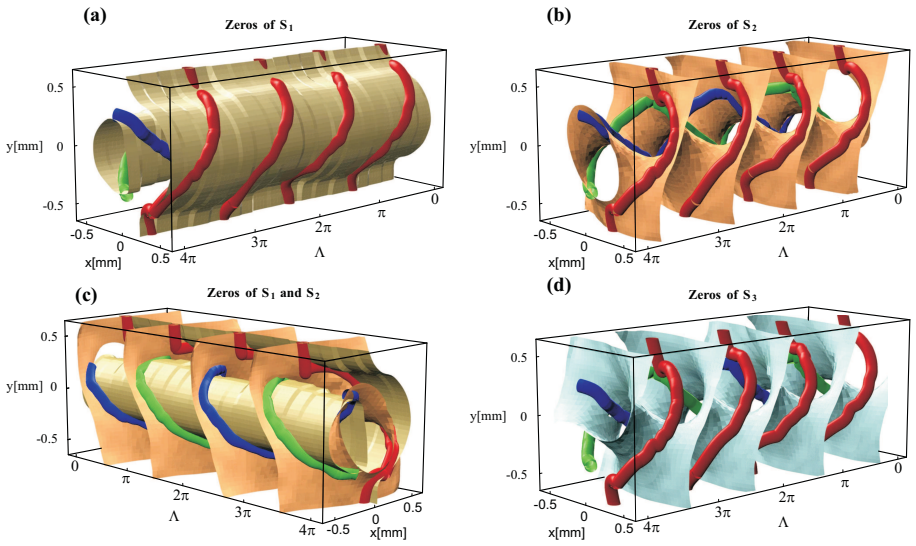

Fig. 5. Experimentally-determined zero surfaces of the Stokes parameters in x,y,Λ-space, and polarization singularities, for an input field with a strength 1 vortex. (a) Surface $S_1 = 0$, with C lines plotted on the surface. (b) Surface $S_2 = 0$, with C lines on surface. (c) Surfaces $S_1 = S_2 = 0$, with C lines along the intersection. (d) L surface ($S_3 = 0$), with C lines off surface. The $S_1 = 0$ surface is invariant with respect to Λ, and the $S_2 = 0$ and $S_3 = 0$ surfaces are the same up to a quarter Λ-period, and are topologically Riemann's minimal surface.

The experimentally-determined zero surfaces of the Stokes parameters, in x,y,Λ-space, are plotted in Fig. 5. The surface for $S_1 = 0$ consists of a tube and a nearby sheet. The periodic surfaces $S_2, S_3 = 0$ are identical, and topologically the same as Riemann's periodic minimal surface [17]. The two surfaces intersect at $(x,y) = (\pm s, 0)$, i.e. at the position of the shifted vortex in each of the two waves. Although topologically the same as Riemann's example, using the expressions in Eq. (5), it can be shown that the surfaces are not themselves minimal (i.e. the mean curvature does not vanish everywhere [21]). The intersection of the translation-invariant $S_1 = 0$ surface with the surface $S_2 = 0$ gives rise to the C line geometry described in Ref. [16]: a double helix of C lines of opposite index and handedness (lying on the $S_1 = 0$ tube) and a transversally infinite C line (lying on the $S_1 = 0$ sheet). If β_{in} changes (this is the angle of the polarization if $\mathbf{d}_{\text{in}}$ is linearly polarized), the $S_2, S_3 = 0$ surfaces do not change, but the S_1 surface does; in particular, when $\beta_{\text{in}} = 45^\circ$, and the C lines reconnect, the S_1 surface and tube touch along two self-intersection lines.

As described in Ref. [16], the complicated polarization singularity geometry in the previous example may be explained as the unfolding of the input optical vortex of the scalar field. When there is no vortex input, the polarization pattern is somewhat simpler. For instance, with a simple Gaussian beam as input, with $\psi_0 = \exp(-(x^2+y^2)/w_0^2)$, the equations for the zeros of the Stokes parameters are

$$\left.\begin{array}{lll} S_1: & x & = [w_0^2 \log\tan^2\beta_{\text{in}}]/8s \\ S_2: & \cos\Lambda & = 0 \\ S_3: & \sin\Lambda & = 0 \end{array}\right\} \text{Gaussian beam input.} \qquad (6)$$

(Similar assumptions are made here as with Eq. (5): δ_{in} is assumed to be zero, and $\sin 2\beta \neq 0$.) The Λ-invariant S_1 surface is just a single plane with constant x, the S_2 and S_3 surfaces are

#75617 - $15.00 USD Received 29 September 2006; revised 31 October 2006; accepted 31 October 2006

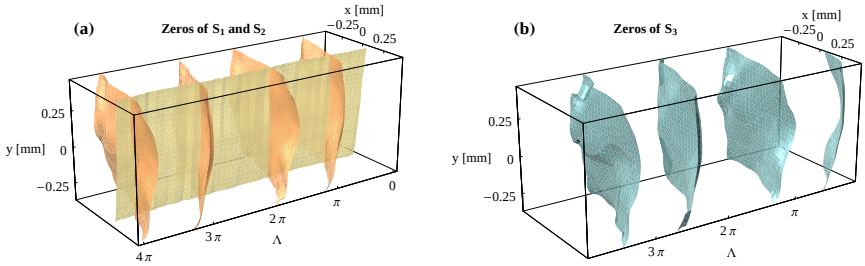

Fig. 6. Zero surfaces of the measured Stokes parameters in x,y,Λ-space, and polarization singularities, for an input field with an input Gaussian (no vortices). (a) Surfaces $S_1 = 0$ (consisting of a single sheet with constant x), and surfaces $S_2 = 0$, corresponding (approximately) to planes of constant Λ. The two sets of surfaces intersect along C lines. (b) L surfaces ($S_3 = 0$), corresponding (approximately) to planes of constant Λ.

planes occurring at constant Λ. Thus the output polarization field has Λ-layers alternating in handedness, with a single C line between two adjacent L surfaces. Since the C line lies in the transverse x,y-plane, its index is not defined [3], although its handedness is. There is no singularity structure threading through the pattern, reflecting the fact that there was no scalar vortex in the input field. The experimentally-determined zeros of S_1, S_2, S_3 for an input Gaussian beam are plotted in Fig. 6.

The input field can be modified to a Laguerre-Gauss beam LG_0^n with any topological charge n (assumed positive here for simplicity), i.e. $\psi_n(x,y) = (x+iy)^n \exp(-(x^2+y^2)/w_0^2)$. In this case, the zeros of the Stokes parameters $S_1 \ldots S_3$ are given by:

$$\left.\begin{array}{lll} S_1: & \frac{(x-s)^2+y^2}{(x+s)^2+y^2}\exp(8sx/nw_0^2) & = \tan^{2/n}\beta_{\mathrm{in}} \\ S_2: & x^2+(y-s\cot([\Lambda+2\pi(m+\frac{1}{4})]/n))^2 & = s^2\,\mathrm{cosec}^2([\Lambda+2\pi(m+\frac{1}{4})]/n) \\ S_3: & x^2+(y-s\cot([\Lambda+2\pi m]/n))^2 & = s^2\,\mathrm{cosec}^2([\Lambda+2\pi m]/n) \end{array}\right\} \quad (7)$$

$$m = 0,1,\ldots,n-1, \qquad \text{charge } n \text{ vortex input.}$$

This expression generalizes Eqs. (5) (when $n = 1$), and, with appropriate limits, (6) (when $n = 0$). The zero contour for S_1 is topologically the same as the $n = 1$ case described above, and the factor $1/n$ just scales the beam waist w_0. However, there are differences in the zero contours of S_2 and S_3. Although the sections of constant Λ are again circles, for each constant Λ there are now n distinct solutions, resulting in exactly n circles with different radii and centers. The corresponding surfaces are the same as those in the $n = 1$ case, but occur with an n-fold multiplicity whilst being shifted in the Λ-direction and intersecting each other in a highly non-generic and unstable way.

For $n = 2$, the Stokes parameter zero surfaces are plotted in Fig. 7, both experimentally (7(a)) and theoretically (7(b)). There are now six C lines, with four coiling around each other, with an overall pitch of 4π instead of 2π.

An alternative representation of the polarization uses the ratio of Cartesian components of $\mathbf{E}$, equivalent to stereographic projection of the Poincaré sphere in the positive S_1-direction, rather than the S_3 direction, as is more usual [18, 13],

$$\rho = \frac{E_y}{E_x} = \frac{S_2+iS_3}{S_0+S_1} = \exp(i\Lambda)\frac{d_{\mathrm{in},y}}{d_{\mathrm{in},x}}\frac{\psi(x+s,y)}{\psi(x-s,y)} = \exp(i[\Lambda+2\delta_{\mathrm{in}}])\tan 2\beta_{\mathrm{in}}\frac{\psi(x+s,y)}{\psi(x-s,y)}. \quad (8)$$

All information about the polarization state is expressed by ρ; in particular, the Stokes zero

#75617 - $15.00 USD Received 29 September 2006; revised 31 October 2006; accepted 31 October 2006

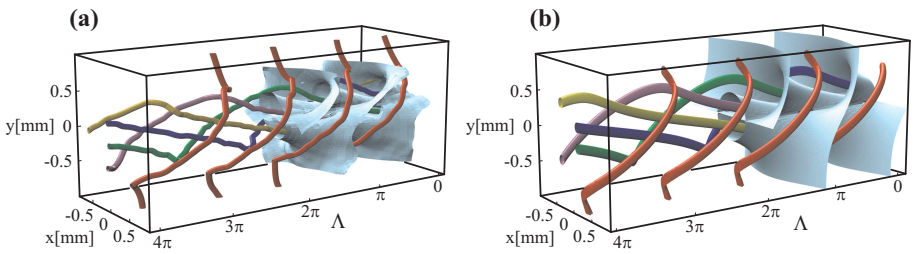

Fig. 7. C lines (intersection of $S_1, S_2 = 0$ surfaces) and L surface ($S_3 = 0$) in x, y, Λ-space, for an input field with a strength 2 vortex. (a) Experimental plot. (b) Theoretical plot. The theoretical L surface corresponds to two intersecting Riemann minimal surfaces. The reconstruction of the self-intersections in the experiment is very sensitive to experimental imperfections.

contour surfaces are specified by $\mathrm{Re}\rho = 0$ ($S_2 = 0$), $\mathrm{Im}\rho = 0$ ($S_3 = 0$), and $|\rho| = 1$ ($S_1 = 0$), and ρ has a zero or pole at the positions of the refracted vortices of the input field.

When the incident field has a regular Gaussian profile (possibly with n axial vortices embedded), the Gaussian factor gives rise to a factor of $\exp(-4xs/w^2)$; for the field ψ_{01}, this is multiplied by $(x+s+iy)^n/(x-s+iy)^n$.

Several general observations can now be made, working with the Poincaré sphere of Stokes parameters, with the non-usual convention of S_1 as the axis of polar coordinates (i.e. with polar angles $2\beta, 2\delta$). S_1 has this privilege as the crystal eigenpolarizations have $S_1 = \pm S_0, S_2, S_3 = 0$. The behavior of all incoming polarizations with the same $\beta (= \arctan|d_{\mathrm{in},y}/d_{\mathrm{in},x}|)$ on the Poincaré sphere is the same. Also, the surface locus of polarizations lying on any great circle including the S_1-direction is the same as the surfaces $S_2 = 0, S_3 = 0$, up to a phase shift (corresponding to a surface $\mathrm{Re}\rho\exp(-i\chi)$ for some phase angle χ). Finally, the loci of any pair of orthogonal polarizations corresponding to opposite points on the great circle perpendicular to the S_1-direction will be the same as the C lines, again up to a phase shift.

3. Discussion

The unfolding of an optical vortex on propagation through a crystal, as explained here and in Ref. [16], demonstrates the interplay between optical vortices, the singularities of scalar optics, and C lines and L surfaces, the singularities of paraxial polarization optics. The effects described occur due to birefringence, and the resulting resolution of polarization, beam walk-off, and phase shift of the two rays; although we have emphasized the situation for uniaxial crystals, the only difference for biaxial crystals is that neither eigenpolarization corresponds to the direction of ray separation (walk-off). Of course, crystal optics has its own singularities [13, 14], particularly when the incoming ray direction coincides with an optic axis of the crystal; the question of how a vortex-carrying beam incident on the optic axis of a crystal is diffracted is outside the scope of the present work. Our experiment can be thought of as the reverse experiment of that described in Ref. [22], in which an optical vortex beam is synthesized from a polarization singularity in the pattern generated from propagation through a crystal (near the optic axis).

The periodicity of the phase shift Λ between the two rays is reminiscent of propagation-periodicity elsewhere in singular optics. As observed in Ref. [16], the configuration of polarization singularities here resembles the braided vortex lines of Ref. [23]. It is natural to ask whether, with an appropriate choice of input field, birefringence alone can produce braided C lines. However, the following argument shows that a pigtail braid of three C lines, as constructed

#75617 - $15.00 USD Received 29 September 2006; revised 31 October 2006; accepted 31 October 2006

for vortices in Ref. [23], is not possible. C lines occur at the intersection of the surfaces $S_2 = 0$ and $S_1 = 0$. Since the latter must be independent of Λ, a (pigtail) braid requires a transverse section of this surface to be a figure-8 [23]. However, such a braid consists of three filaments, requiring the $S_2 = 0$ surface to cross the Λ-invariant $S_1 = 0$ surface three times for each Λ. This is clearly impossible, as contour surfaces intersect generically an even number of times, proving that braided C lines are impossible using Eq. (3).

A common example of perturbing an optical vortex is the superposition of a screw dislocation with a copropagating plane wave of small amplitude [1, 6], in which the straight vortex line becomes helical. The situation we describe is a generalization of this in two ways [24]. Firstly, the superposition of Eq. (3) is a superpositions of waves with orthogonal polarizations, rather than (implicitly) the same polarization, so the final pattern involves polarization singularities rather than phase singularities. Secondly, there is a vortex in each of the fields being superposed. If two orthogonally polarized beams were superposed, one with a vortex, the other a plane wave (with a phase shift Λ), then the zero contours of the Stokes parameters are a cylindrical tube invariant with Λ ($S_1 = 0$), and a pair of orthogonal helicoids along the same axis ($S_2, S_3 = 0$): this results in a double helix of C lines with opposite sign and handedness. Although illustrative, this example cannot be physically realized in an experiment involving crystal birefringence, as both fields must be the same up to a spatial and phase shift.

A further generalization of the effect described here would be to extend to crystals which possess optical activity or absorption (dichroism) [13]. In these cases, we do not anticipate the rich polarization topology of pure birefringence to occur. The dielectric tensor of an optically active crystal is complex Hermitian, and the orthogonal eigenpolarizations for a non-singular propagation direction are in general elliptic. The behavior of the zero contours for generalized Stokes parameters, based on an orthogonal triad of polarizations on the Poincaré sphere (with one direction corresponding to the eigenpolarizations), is the same as that described in Section 2 for birefringent crystals without optical activity; however, the polarization singularities (C lines, L surfaces) do not possess the geometry described in Section 2 because the usual Stokes parameter triad describing them has no relationship to this generalized triad based on elliptic polarizations. Dichroic crystals do not, in general, have orthogonal eigenpolarizations, so the decomposition (3) fails.

The discussion at the end of Section 2, as well as the previous paragraph, implies that there is nothing special about the polarization state on C lines and L surfaces. Of course, from the viewpoint of the Poincaré sphere this may be true; however, the approach of singular optics is to deduce properties of the entire optical field from the behavior of the singularities, possible due to their geometrically singular nature (the polarization at a C line is rotationally invariant, the handedness on an L line is not defined). The remarkable properties of Stokes parameters and the Poincaré sphere remove this specialness, but only in the abstract, three-dimensional Stokes space: the geometric fine structure of the spatially inhomogeneous polarization field we describe is completely physical.

Acknowledgements

UTS acknowledges support from the Japan Society for the Promotion of Science (JSPS), and MRD acknowledges support from the Royal Society of London.

#75617 - $15.00 USD Received 29 September 2006; revised 31 October 2006; accepted 31 October 2006